Journal of Heat and Mass Transfer Research 8 (2021) 127- 138

Journal of Heat and Mass Transfer Research

Journal homepage: http://jhmtr.semnan.ac.ir

Semnan University

The Effects of Operational Parameters on the Flow Characteristics in Annular Space During Under-Balanced Drilling Operations

Saeed Ghobadpouri [*,a], Ali Falavand Jozaei[b]

[a] *Mechanical Engineering Department, Faculty of Gas and Petroleum (Gachsaran), Yasouj University, Gachsaran 75813-56001, Iran.*
[b] *Department of Mechanical Engineering, Ahvaz Branch, Islamic Azad University, Ahvaz, Iran.*

PAPER INFO

Paper history:
Received: 2021-01-27
Revised: 2021-05-15
Accepted: 2021-05-15

Keywords:
Under-Balanced Drilling;
Operational Parameters;
Flow Characteristics.

ABSTRACT

In this research, gas-liquid-solid three-phase flow in the annulus during under-balanced drilling operations is simulated numerically. One-dimensional form of steady-state governing equations including mass and momentum conservation equations for each phase, gas equation of state, and saturation constraint equation in the Eulerian frame of reference are solved by a proposed algorithm. The computational code is validated by using experimental data from a real well, gas-liquid two-fluid numerical simulation, and also some mechanistic models of WellFlo software. Moreover, the results are compared with the experimental data from a laboratory study. The numerical code succeeds in predicting bottom hole pressure and obtaining the characteristic flow behavior during under-balanced drilling. Due to the importance of controlling flow characteristics during the drilling operations, the effects of change in the injected liquid flow rate, gas injection flow rate, choke pressure on the gas, liquid, and solid volume fractions, as well as gas, liquid, and solid velocity distributions along with the annulus, are investigated. According to the obtained results, the effects of liquid injection flow rate and injected gas flow rate on the flow characteristics are decreased along the annulus in the flow direction, but the effects of choke pressure on the flow characteristics are increased along the annulus in the flow direction. Consequently, to change the flow characteristics in the wellhead area, it is better to change the choke pressure and to affect the flow characteristics in the bottom-hole area, it is preferred to change the gas and liquid injection flow rate. In other words, depending on the required situation of flow characteristic changes, the appropriate operational parameter can be used.

DOI: 10.22075/JHMTR.2021.22474.1331

1. Introduction

Two important pressures during drilling operations are the pressure due to the drilling fluid and the formation pressure. Different drilling techniques are defined based on the comparison between these two pressures. The most common method of drilling is over- balanced drilling (OBD). In OBD, the drilling fluid pressure is higher than the pressure of the formation that leads to cuttings and drilling fluid penetrate into formation. This phenomenon results in the drilling fluid to be wasted, the formation to be damaged, and the production of wells to be reduced. If the drilling fluid pressure is kept below the formation pressure, the drilling technique is called under-balanced drilling operation (UBD). In UBD operation, the drilling fluid does not penetrate into the reservoir due to its lower pressure than the pressure of the formation, so the problem of damage to the formation is solved. In addition, in UBD operations, bit life, bit penetration rate, and drilling velocity are higher than OBD. Moreover, hydrocarbon extraction can be started from the reservoir at the same time as the drilling operation and as soon as it enters an exploitable area.

During UBD operations, by simultaneous injecting gas-liquid two-phase flow to the drill pipe and controlling the outlet pressure at the wellhead (choke pressure), the bottom hole pressure (BHP) is maintained in a desired range. This pressure range is called "the pressure window". The upper limit of the pressure window is the reservoir pressure and its lower limit is restricted with collapse pressure. The injected gas-liquid two-phase flow from the wellhead is passed through the drill pipe and bit

[*]*Corresponding Author: Saeed Ghobadpouri, Mechanical Engineering Department, Faculty of Gas and Petroleum (Gachsaran), Yasouj University, Gachsaran 75813-56001, Iran.*
Email: ghobadpouri.s@yu.ac.ir

and then is entered the bottom hole. At the bottom hole, drill cuttings are added to this two-phase flow and consequently, gas- liquid- solid three-phase fluid is flowing from the bottom to the wellhead along the annulus. To design successful drilling operations and desired well condition controlling, having sufficient information about the effect of each operational parameter on the annulus fluid flow characteristics is essential.

One of the most comprehensive researches with a numerical approach has been conducted in Bergen, Norway. The presented software called Dyna Flo Drill [1-5]. In this software, the momentum equation is simplified and it is assumed that the velocity of all phases is the same. This software predicts flow parameters in some cases with an error almost close to 100%. Fan et al. [6] presented a dynamic model to predict the multi-phase drilling fluid flow behavior in the UBD operations. This study also used a general momentum equation for all phases which is not accurate enough to predict the phases velocity distribution. Perez-Tellez [7] and Perez-Tellez et al. [8] used drift flux model and proposed a numerical code to simulate gas-liquid two-phase flow in UBD operation. In this study, the effects of drill cuttings have not been considered and due to the use of the drift flux model, a weakness in predicting the velocity distribution of some two-phase flow regimes such as slug is observed. The cuttings volume fraction effects on the continuous flow inside a vertical pipe was studied using a mechanistic model by Fadairo and Falode [9]. Based on this research, drill cuttings can delay the flow of fluid lead to increase in BHP and equivalent density of drilling fluid. Yan et al. [10] had an overview of the empirical correlations, mechanistic models, and sensitivity analyses for cuttings transport with aerated liquid during UBD. Based on this research, during UBD the main operational parameters which affect aerated liquid characteristics are fluid flow rate and rheology. In the conclusion of this article, the need to further study on the flow simulation has been emphasized. Effects of operational parameters on BHP during UBD operations are investigated numerically by Ghobadpouri et al. [11]. In this research, the effects of operational parameters on the velocities of the phases, gas and liquid void fractions have not been represented. Also, the effects of oil and gas production in boundary conditions and the algorithm solution process are not considered. Wei et al. [12] developed a model and a computational code for gas-liquid two-phase flow. This simulation used a general mixture momentum conservation equation for all phases led to erroneous results in velocities prediction. Li et al. [13] developed a model to predict the horizontal well's maximum allowable measured depth during UBD operation. This model is designed based on the dynamic bottom-hole pressure balance to maintain the under-balanced state. In this research, the hole-cleaning problems were not considered.

During drilling operations, flow rates of the injected liquid and injected gas from the wellhead besides the choke pressure at the outlet of the annular space can be adjusted by the drilling engineer to control the drilling process. Changing theses operational parameter affect annulus flow characteristics. Proper use of these parameters to achieve the successful drilling, requires sufficient knowledge of how each of the parameters affects the characteristics of the drilling fluid flow. The studies of previous researches show that less attention has been paid to investigate the effects of operational parameters on the flow characteristics. Most of the previous researches in the UBD operation focused on the study of the effects of operational parameters on BHP. Meanwhile, the hole-cleaning problem is controlled by means of studying the velocities and the volume fraction distribution of liquid and solid phases along the annulus. Proper use of different operational parameters to apply the desired changes in a specific location is one of the advantages of this study. Besides, studying the effects of operational parameters on flow characteristics such as phases velocity and volume fraction, improve physical insights into the problem and help to design successful drilling operations. Therefore, in the present study the effects of operational parameters on multi-fluid flow characteristics, including the volume fraction of different phases and the velocity of each phase, have been investigated.

As far as we know, this paper is the first research in which the effects of operational parameters including gas flow rate, liquid flow rate, and choke pressure on the characteristics of gas-liquid-solid three-phase flow are investigated using numerical approach. For this purpose in fallows, the governing equations are provided in section 2. Then, the implemented algorithm and numerical solution approach are represented. In section 3, developed code is validated using the available experimental data, field data and also some numerical and mechanistic solution from other research. Then, the effects of the injected gas flow rate, the injected liquid flow rate, and the outlet pressure (choke pressure) on distribution of the gas, liquid, and solid volume fraction and its velocities are investigated. Finally, in Section 4 the conclusions are provided.

2. Governing equations

During UBD operations, each of the liquid and gas phase inside the annular space consists of two components. As shown in Fig. 1, one of these components is injected from the wellhead into the drill pipe and after passing through the bit enters the annular space. The second component, flows from the formation into the annulus. Usually, these components are two fluids with different properties.

In this research, it has been assumed that only a single-hypothetical liquid and a single- hypothetical gas besides cuttings flow inside the annular space.The required properties of these hypothetical fluids are calculated based on the weighted average of the components. Due to the large length of the drilled depth in comparison with the diameter of the drill pipe, it is assumed that the geometry of the problem is one-dimensional.

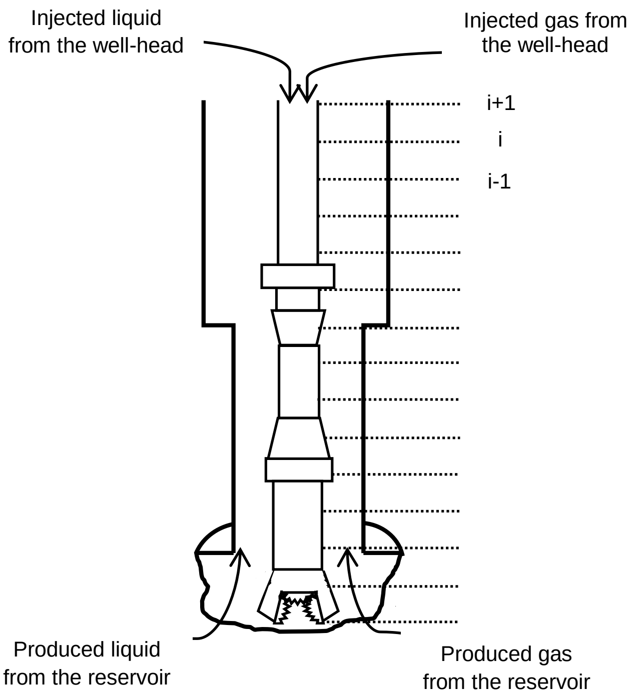

Figure 1. Fluid flow in the annular space during UBD operations.

Due to the large length of the drilled depth in comparison with the diameter of the drill pipe, it is assumed that the geometry of the problem is one-dimensional. The temperature distribution along the well is considered to be the same as the geothermal distribution. Here, it is considered that the liquid phase is incompressible, and the gas phase is to be compressible. Thus, the governing equations will be as follows [14-15].

$$\frac{d}{dx}(\alpha_G\rho_G u_G A) = 0 \tag{1}$$

$$\frac{d}{dx}(\alpha_L\rho_L u_L A) = 0 \tag{2}$$

$$\frac{d}{dx}(\alpha_S\rho_S u_S A) = 0 \tag{3}$$

$$\begin{aligned}\frac{d}{dx}(\alpha_G\rho_G u_G^2 A) = -A\Big(F_{iG} + F_{wG} + F_{gG} \\ + F_{vG} + \alpha_G\frac{\partial P}{\partial x}\Big) \\ - \Delta P_{iG}\frac{d(A\alpha_G)}{dx}\end{aligned} \tag{4}$$

$$\begin{aligned}\frac{d}{dx}(\alpha_L\rho_L u_L^2 A) = -A\Big(F_{iL} + F_{wL} + F_{gL} \\ + F_{vL} + \alpha_L\frac{\partial P}{\partial x}\Big) \\ - \Delta P_{iL}\frac{d(A\alpha_L)}{dx}\end{aligned} \tag{5}$$

$$\begin{aligned}\frac{d}{dx}(\alpha_S\rho_S u_S^2 A) = -A\Big(F_{iS} + F_{wS} + F_{gS} \\ + F_{vS} + \alpha_S\frac{\partial P}{\partial x}\Big)\end{aligned} \tag{6}$$

Since the flow is steady-state with no phase change, the mass flows must be constant along the entire annulus. By utilizing a forward first order approximation for the spatial derivatives and use constants K_{Gin}, K_{Lin} , K_{Sin} for defining the inlet gas, liquid and solid boundary conditions, the governing equations in the discretized form will be as follows

$$(\alpha_G\rho_G u_G A)_i = K_{Gin} \tag{7}$$

$$(\alpha_L\rho_L u_L A)_i = K_{Lin} \tag{8}$$

$$(\alpha_S\rho_S u_S A)_i = K_{Sin} \tag{9}$$

$$\begin{aligned}K_{Gin}\big(u_{G,i+1} - u_{G,i}\big) \\ = -A_i\alpha_{G,i}(P_{i+1} - P_i) \\ - \Delta P_{iG}((A\alpha_G)_{i+1} \\ - (A\alpha_G)_i) - \Delta x A_i S_{G,i}\end{aligned} \tag{10}$$

$$\begin{aligned}K_{Lin}\big(u_{L,i+1} - u_{L,i}\big) \\ = -A_i\alpha_{L,i}(P_{i+1} - P_i) \\ - \Delta P_{iL}((A\alpha_L)_{i+1} \\ - (A\alpha_L)_i) - \Delta x A_i S_{L,i}\end{aligned} \tag{11}$$

$$\begin{aligned}K_{Sin}\big(u_{S,i+1} - u_{S,i}\big) \\ = -A_i\alpha_{S,i}(P_{i+1} - P_i) \\ - \Delta x A_i S_{S,i}\end{aligned} \tag{12}$$

In these equations, u is velocity, α is volume fraction, P is pressure, and ρ is density. G, L, and S subscripts are used to identify gas, liquid, and solid phases, respectively. $S_{K,i} = F_{iK} + F_{wK} + F_{gK} + F_{vK}$; $(K = G, L, S)$where $F_{iK}(k = G, L, S)$ is the drag force exerted on phase k as a result of the interaction of the other phases. The drag force is the most significant force exerted on the phases [16]. The effect of annulus walls on the fluid flow is considered as a source term in the momentum equations [17]. The frictional force of the wall is represented by $F_{wK}(k = G, L, S)$. $F_{gK}(k = G, L, S)$ is the force of gravity and $F_{vK}(k = G, L, S)$ denotes the virtual mass force. ΔP_i is the pressure correction term. Modeling of the above-mentioned forces, the pressure correction term, flow patterns and also pattern recognition criteria presented in Hatta et al[15].

There are eight unknowns in the above equations. The independent variables are all the fractions, the velocities, the gas density, and the pressure, eight variables in total. So, besides the mass and momentum conservation equations, two other equations are needed to close the system. The first one is saturation constraint which expresses that the sum of all volume fractions must be the one to fill the cross section.

$$\sum_{k} \alpha_k = \alpha_G + \alpha_L + \alpha_S = 1 \tag{13}$$

The next equation is the gas phase equation of state.

$$\rho_G = \rho_G(P_G, T_G) = \frac{M_G \cdot P}{8314 \cdot Z \cdot T} \tag{14}$$

The compressibility factor of the gas phase (Z) is found from the Equation 15 which is proposed by Dranchak and Abou-Kassem[18]

$$\begin{aligned} z &= \left(0.3265 - \frac{1.0700}{T_{pr}} - \frac{0.5339}{T_{pr}^3} + \frac{0.01569}{T_{pr}^4} - \frac{0.05165}{T_{pr}^5}\right)\rho_r \\ &+ \left(0.5475 - \frac{0.7361}{T_{pr}} + \frac{0.1844}{T_{pr}^3}\right)\rho_r^2 \\ &- 0.1056\left(-\frac{0.7361}{T_{pr}} + \frac{0.1844}{T_{pr}^3}\right)\rho_r^5 \\ &+ 0.6134(1.0 + 0.7210)\rho_r^2 \frac{\rho_r^2}{T_{pr}^3} \exp(-0.721\rho_r^2) + 1.0 \end{aligned} \tag{15}$$

where ρ_r is reduced density and

$$\rho_r = \frac{0.27P_{pr}}{ZT_{pr}} \tag{16}$$

Also $T_{pr}$is reduced temperature and P_{pr} is reduced pressure. Where

$$T_{pr} = \frac{T}{T_{cr}} \tag{17}$$

$$P_{pr} = \frac{P}{P_{cr}} \tag{18}$$

2.1. Solution method

The governing equation, including continuity and momentum equations for each phase (Eqs. (1) –(6)), the saturation constraint (Eq. 13), and gas phase equation of state (Eq. 14) form a coupled system of ordinary differential equations (ODE). There are 8 equations with 8 unknowns. The governing equations are discretized by utilizing a forward first order approximation for the spatial derivatives. We would be able to construct a recursive solution scheme based on the Newton iterative method to solve this algebraic system of coupled nonlinear equations. The governing equations in discrete form can be represented in the following matrix.

$$F = \begin{bmatrix} F_1 \\ F_2 \\ F_3 \\ F_4 \\ F_5 \\ F_6 \\ F_7 \\ F_8 \end{bmatrix} = \begin{bmatrix} \left(\alpha_G \rho_G u_G A\right)_i - K_{Gin} \\ \left(\alpha_L \rho_L u_L A\right)_i - K_{Lin} \\ \left(\alpha_S \rho_S u_S A\right)_i - K_{Sin} \\ K_{Gin}\left(u_{G,i+1} - u_{G,i}\right) + \alpha_{G,i} A_i (P_{i+1} - P_i) + \\ \dots A\Delta P_{iG}\left(\alpha_{G,i+1} - \alpha_{G,i}\right) - \Delta X \cdot A_i \cdot S_{G,i} \\ K_{Lin}\left(u_{L,i+1} - u_{L,i}\right) + \alpha_{L,i} A_i (P_{i+1} - P_i) + \\ \dots A\Delta P_{iL}\left(\alpha_{L,i+1} - \alpha_{L,i}\right) - \Delta X \cdot A_i \cdot S_{L,i} \\ K_{Sin}\left(u_{S,i+1} - u_{S,i}\right) + \alpha_{S,i} A_i (P_{i+1} - P_i) - \\ \dots \Delta X \cdot A_i \cdot S_{S,i} \\ \alpha_G + \alpha_L + \alpha_S - 1.0 \\ \rho_{G,i} - \rho(P_i, T_i) \end{bmatrix} = \begin{bmatrix} 0 \\ 0 \\ 0 \\ 0 \\ 0 \\ 0 \\ 0 \\ 0 \end{bmatrix} \tag{19}$$

2.2. Boundary conditions and problem solving algorithm

The governing equations are 8 equations with 8 unknowns. We seek to determine all the fractions (three variables), the velocities (three variables), the gas density (one variable), and the pressure (one variable), eight independent variables in total. Boundary conditions (B.C.) which imposed to the solution method are constant mass flows for gas, liquid and solid at the inlet (three B.C.), the given drilling velocity at the inlet of the annulus (one B.C.), Saturation constraint which must be satisfied at both the inlet and outlet (two B.C.), the choke pressure which is directly inserted as outlet pressure (one B.C.). The gas density at the outlet which can be obtained using the gas equation of state and choke pressure and also the temperature at the wellhead according to the gas phase equation of state (one B.C.).

The steady state gas- liquid- solid three-phase flow in the annulus during UBD operation is simulated numerically using the following steps:

1. The calculations start from the wellhead (above the annular space) and continue along the annulus until reaching the bottom hole.
2. The first iteration loop begins with guessing the amount of produced oil and gas from the reservoir. It

is initially assumed that oil and gas are produced in the maximum possible amount. Using these values as well as the injected flows of the liquid and gas phases from the wellhead, the equivalent properties of the liquid and gas phases in the annular space are calculated based on the weighted average of the components.

3. Solid phase density, drilling velocity and average diameter of drill cuttings are taken as input.
4. The pressure at the outlet of the annular space is equal to the choke pressure. Using the equation of state of the gas phase, choke pressure, and temperature in the wellhead, the gas phase density at the annulus outlet is calculated.
5. The second iteration loop starts with guessing the volume fractions of the gas and solid phases at the wellhead node. Using these assumed values and algebraic constraint equations, the volume fraction of the liquid phase at the wellhead is calculated. Using these values and three-phase mass conservation equations, the velocities of the solid, liquid and gas phases in the wellhead node are determined. Thus, in steps 4 and 5, all unknowns are identified in node i+1 Fig. 1.
6. The third iteration loop starts with guessing the unknown independent variables in the second node from the wellhead (node i in Fig. 1). These assumed values are modified using the Newton iterative procedure $\left(\mathrm{Y}_{\mathrm{n+1}} = \mathrm{Y}_{\mathrm{n}} - \mathrm{J}^{-1}\mathrm{F}_{\mathrm{n}}(\mathrm{Y}_{\mathrm{n}})\right)$. In this procedure Y is unknown vector that consists of the independent variables. The independent variables are all the fractions (three variables), the velocities (three variables), the gas density (one variable), and the pressure (one variable), eight variables in total. F is obtained from Equation 19 using the values in a wellhead node (node i+1 in Fig. 1) and the second node from the wellhead (node i Fig. 1). $\mathrm{J}^{-1}$is the inverse of the Jacobi-matrix. The Jacobi-matrix J=∂F⁄∂Y is calculated by investigating how that affects F with slightly varying of each argument [19]. Newton-iteration processes to calculate the modified values of Yi vector are repeated until convergence. Since the F-vector (Eq.19) should end up having zero length, so $\sqrt{\sum_{\mathrm{i=1}}^{8} \mathrm{F_i}^2} < 10^{-7}$ is used as convergence criterion.
7. As in step 6, the solution process repeated from the downstream (wellhead) to the upstream (bottom of the well) for other nodes. If we made a poor guess regarding outlet value at the wellhead node for the volume fractions of the gas and solid phases, we are still going to approach the correct values. The inaccurate outlet values will appear as abrupt changes in the fractions. We can use volume fraction values some distance into the outlet which are more accurate to extrapolate to the outlet values. Accordingly, better starting values are gained and do a rerun of the calculations. That procedure can be repeated several times to improve accuracy further until the convergence criteria is satisfied. The convergence criteria which are used is $\left(\left|\alpha_{\mathrm{G,i=1}}^{\mathrm{n+1}} - \alpha_{\mathrm{G,i=1}}^{\mathrm{n}}\right| + \left|\alpha_{\mathrm{L,i=1}}^{\mathrm{n+1}} - \alpha_{\mathrm{L,i=1}}^{\mathrm{n}}\right| + \left|\alpha_{\mathrm{S,i=1}}^{\mathrm{n+1}} - \alpha_{\mathrm{S,i=1}}^{\mathrm{n}}\right| < 10^{-5}\right)$.
8. The solution procedure continues to the bottom hole. Using the BHP and Vogels equation [20], the amount of the produced oil and gas from the reservoir is modified. The solution procedure continues from step 2 with the modified values, until the convergence criteria is satisfied. The used convergence criteria in this step is $(|\mathrm{BHP}^{\mathrm{n+1}} - \mathrm{BHP}^{\mathrm{n}}| < 10^{-7})$.

3. Results and discussions

3.1. Validation

To validate the performance of the developed multi-fluid model code used the information of Muspac-53 well [7], which is an operational vertical well located in Mexico and drilled using the UBD operation. In this well, Nitrogen is injected into the drill pipe as a gas phase at 15.014 m^3/min (530 scfm). The liquid with 0.94 specific gravity at 0.5075 m^3/min (133 gpm) was implemented as a liquid phase drilling fluid. The choke pressure is set to 0.310 MPa (45.12 psi). The simulated depth is 2605m. The average cuttings diameter is assumed to be 6 mm. At the wellhead the surface temperature is 301.15K and the temperature gradient along the annular space is 2.83k/100m. Drilling operation velocity is 6m/hour and the solid density is 2800Kg/m^3. Annulus well geometry information and flow test data of Muspac53 well is represented in table1 and table2 respectively.

Table 1. Muspac-53 Annulus well geometry [7]

Depth (m)	Annuls inner diameter (mm)	Annuls outer diameter (mm)
0-2555	88.9	152.5
2555-2597	120.7	152.5
2597-2605	120.7	149.2

Table 2. Muspac-53 Flow test data [7]

Nitrogen flow rate	15.014 m^3/min (530$Scfpm$)
Injected liquid specific ravity	0.94
Liquid flow rate	0.5075 m^3/min (133gpm)
Choke pressure	0.310 MPa (45.12 Psi)
Simulated depth	2605 m
Average cutting dimeter	6 mm
Wellhead temperature	301.15 K
Temperature gradient along the annulus	2.83 $k/100m$
Drilling velocity	6 $m/hour$
Solid density	2800 kg/m^3

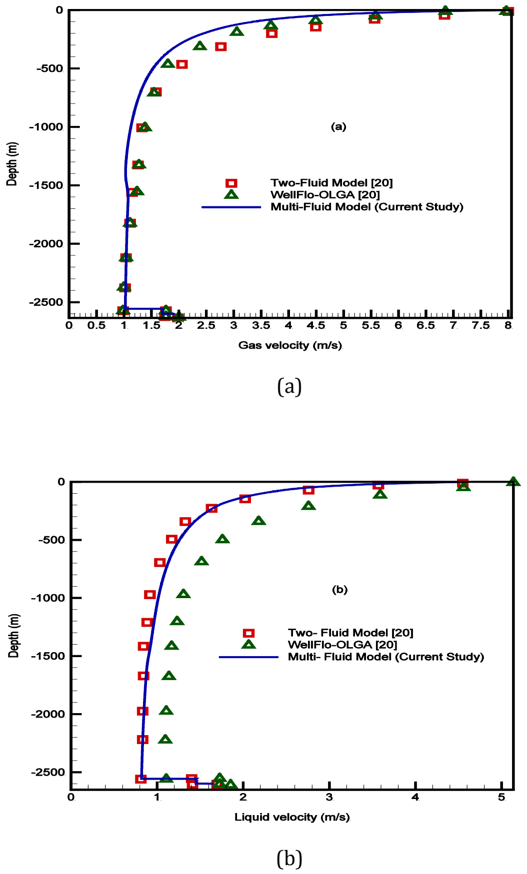

Figure 2. Variation of (a) gas -(b) liquid velocity along the Muspac-53 annulus.

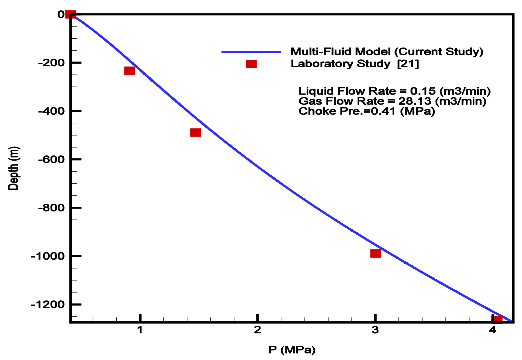

Figure 3. Comparison of pressure variation with Lage and Time laboratory study [22].

In table 3, the obtained BHP of Muspac53 from the current developed multi fluid model, is compared with the result of some mechanistic models, two-phase numerical simulation, and also with the existing field data [7, 21]. As shown in table 3, the gas- liquid- solid multi-fluid model is more accurate than the gas- liquid two-fluid model for BHP. It has better accuracy than the Biggs & Brill, and OLGA model of WELLFLO software. Although the Hassan and Kabir model of WELLFLO software has better accuracy for BHP compare to the gas- liquid- solid multi-

Table 3. Multi-fluid model prediction of Muspac-53 bottom hole pressure comparison against TFM, Wellflo, and field data.

	BHP (MPa)	%Error-BHP
Wellflo-OLGA [22]	16.1320	28.24
Wellflo-Biggs & Brill [22]	16.9146	24.76
Two-Fluid Model [22]	18.7407	16.63
Three-Fluid Model (Current Study)	19.2625	14.31
Wellflo-Hasan & Kabir [22]	20.1755	10.25
Field data [7]	22.4799	-

fluid model, but it should be noted that, this model is a two-fluid model and does not provide any information about cutting distribution along the annular space. Moreover, this model is a mechanistic model based on experimental relationships. Therefore, having more accuracy of this mechanistic model in simulating this particular well, is not a reason for its superiority of accuracy in all conditions and modeling of other wells.

Figs. 2-a and 2-b compare the gas and liquid velocities variation along the annular space were gained using current developed multi-fluid model, gas- liquid two-fluid model and OLGA-WELLFLO software results [21]. According to these figures, the numerical code succeeds in obtaining the velocities variation behavior during under balanced drilling and shows good accuracy in comparison with other research.

Simulation of the multi-fluid flow in the annulus of a laboratory study by Lage and Time [22] also confirms the validity of the current study. This well was 1275-meter-deep. Pressure and temperature distribution along with the annulus are reported by means of the four sensors which is installed at depths of 240, 494, 998, and 1273 meters. The inner and outer diameters of the annular space are 88.9 mm and 159.4 mm respectively. The results were obtained for water injection with 0.15 m^3/min flow rate, nitrogen with 28.13 m^3/min, and choke pressure 0.41 MPa. Fig. 3 shows the annulus pressure variation comparisons for the laboratory study by the Lage and Time [22] and Multi-fluid models. This figure, also confirms the validity of the current study.

3.2. Simulation results

In this section the effects of different operational parameters including choke pressure, the injected gas and liquid flow rates on the flow characteristics are investigated using the current developed multi-fluid model code.

3.2.1. The effects of injected gas flow rate on the annulus flow characteristics

Figs.4 shows the distribution of volume fractions and velocities along the annulus at different gas flow rates,

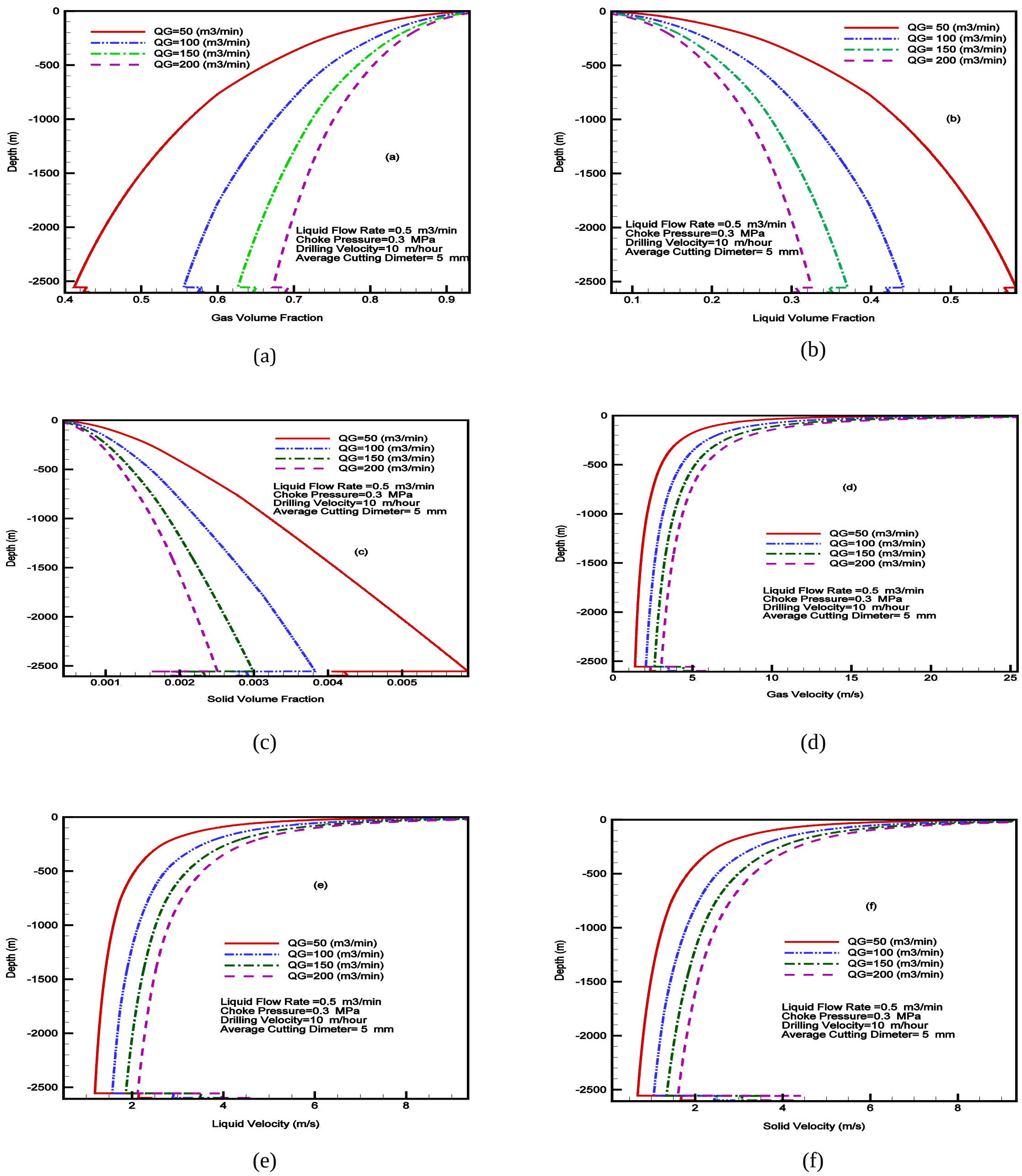

Figure 4. The effects of injected gas flow rate on the annulus flow characteristics.

where liquid flow rate and choke pressure are kept constant. The rapid change in the volume fractions distributions and velocity profiles are due to the rapid diameter changes in the annulus. As shown in Fig. 4-a in regions with uniform cross-sectional area, at a constant injected gas flow rate, the gas volumetric fraction is increasing in the annulus in the flow direction. Furthermore, according to Fig 4-b and Fig 4-c the liquid and solid volume fractions are decreased in the annulus in the flow direction at a constant injected gas flow rate. As the volume flow rate of the gas phase increases, the difference in volume fractions of all phases (gas, liquid and solid) at the bottom of the well and wellhead is decreased. Changing the gas phase flow rate has further changed the volume fractions at the bottom region of the well.

Figs. 4-d, 4-e, and 4-f shows the gas, liquid and solid phase velocity profiles along the annulus. According to these figures, in areas with uniform cross-sections, the velocity of all phases is increased in the annulus in the flow direction at a constant injected gas flow rate. The rates of velocity increases at constant operational parameters are reinforced in the flow direction for all phases. In all phases the highest rate of velocity changes occurs in wellhead area. Also, by increasing the injected gas flow rate, velocities are increased through the annular space. The amount of these changes is more noticeable in the bottom-hole area

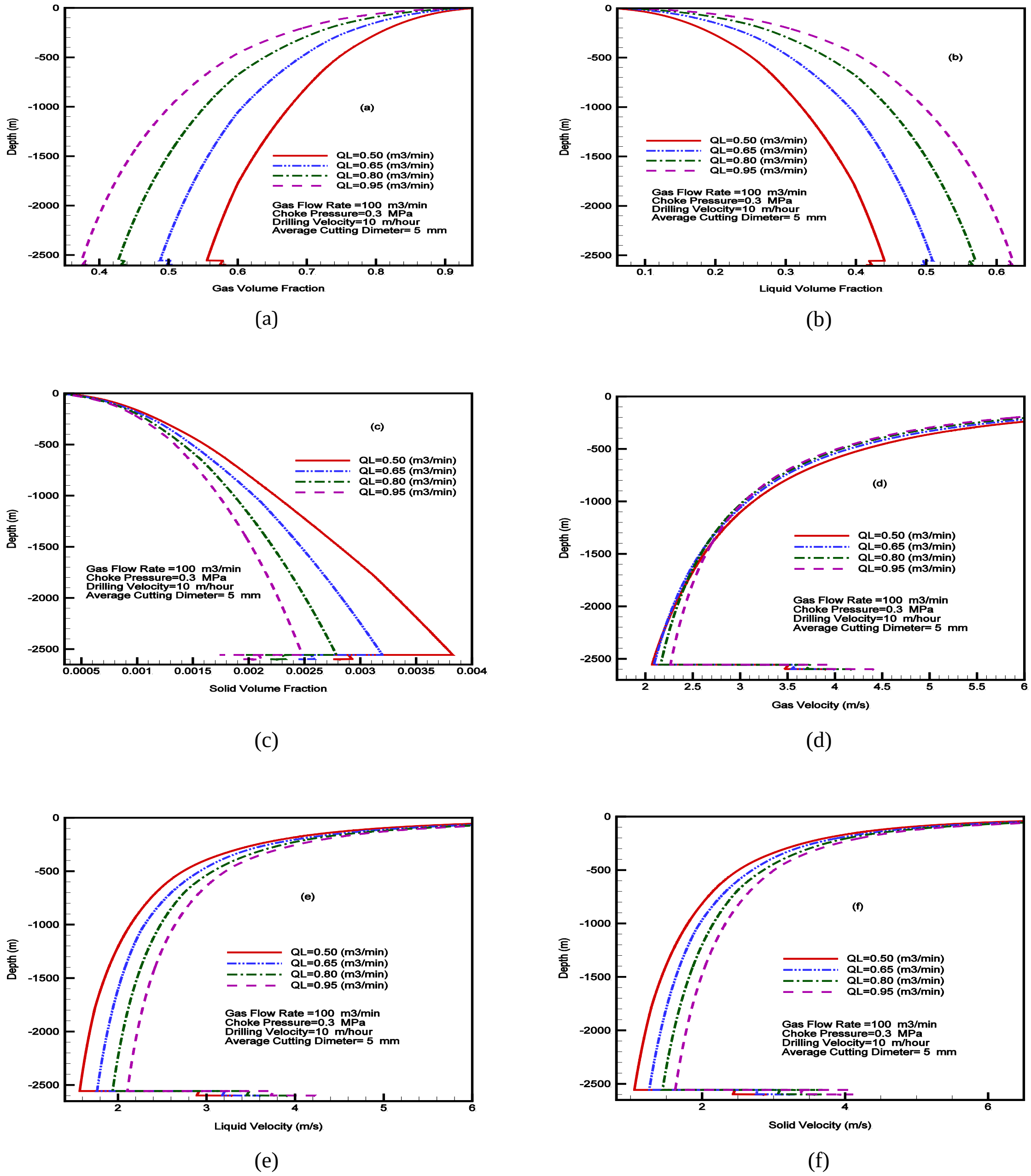

Figure 5. The effects of injected liquid flow rate on the annulus flow characteristics.

3.2.2. The effects of injected liquid flow rate on the annulus flow characteristics

Figs.5 demonstrates the distribution of volume fractions and velocities along the annulus at different liquid flow rates, where gas flow rate and choke pressure are kept constant. As the injected liquid flow rate increased, the volume fractions of the gas phase and solid phase decreased (Figs. 5-a and 5-c) but, the volume fraction of the liquid phase increased (Fig. 5-b). As shown in Figs. 5-d, 5-e, and 5-f, at a constant operational parameter, the highest rate of change of the gas, liquid and solid velocities is in the wellhead area. Moreover, in the bottom hole area, the ratio of velocity changes to the initial velocity (Δu/u) of all phases (liquid, solid and gas) are increased as the flow rate of the injected liquid phase is increased, but in the wellhead area the changes of velocities due to the injected liquid flow rate variations are not tangible.

3.2.3. The effects of injected liquid flow rate on the annulus flow characteristics

In Figs. 6 demonstrates the effects of changing choke pressure on the flow characteristics while gas and liquid flow rate are kept constant. Increasing the choke pressure made an increase in the volume fraction of liquid and solid phases and led to decreases in the volume fraction of the gas phase along the entire length of the annulus. The

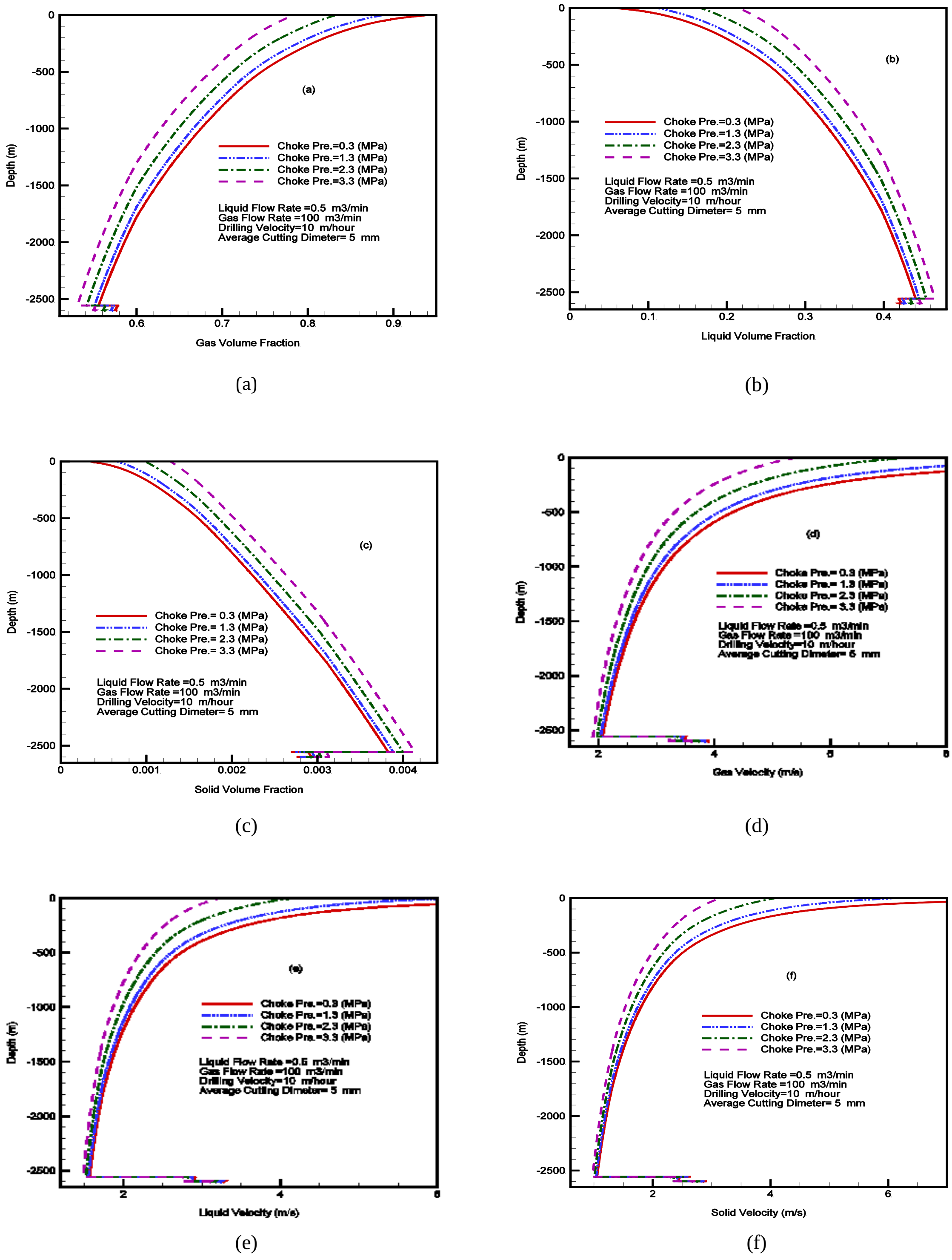

(a) (b) (c) (d) (e) (f)

Figure 6. The effects of choke pressure on the annulus flow characteristics.

velocity of all phases decreases with increasing choke pressure. The effects of choke pressure on the volume fraction and velocity of different phases are more in the wellhead area. These effects in the wellhead area are not perceptible. In other word, the effects of choke pressure on the flow characteristics are increased along the annulus in the flow direction. In fact, as the depth decreases in the flow direction, the hydrostatic pressure becomes smaller and smaller, and the order of choke pressure compared to the total pressure becomes larger, so the effect of the choke pressure on the annulus flow characteristics are increased in the flow direction.

Conclusion

In this study, a numerical approach of single pressure multi-fluid model was used for investigation of the annulus flow characteristics, including phases velocity and volume fraction during the UBD operation. The implemented numerical simulation is shown good accuracy in comparison with the field data, experimental results, gas- liquid two-fluid model (TFM) and some mechanistic models of the WELLFLO software. Effects of injected gas flow rate, injected liquid flow rate and choke pressure on the flow characteristics has been investigated using the developed code. Due to this fact that, during UBD operations, flow regimes from the bottom to the top of the annulus are bubbly, slug and churn, respectively. At the wellhead area, flow regime is slug or churn and the most common phase is the gas phase. In fact, the total pressure is decreased from the bottom to the top of the well in the flow direction. The total pressure along the annulus consists of the frictional and gravitational terms. Gravitational term decreases in flow direction due to decreases of depth. The frictional term due to its acts in the opposite directions of flow causes extra pressures drop due to increase of velocities in the flow direction. On the other hand, the gas phase is most affected by pressure due to its compressibility. Therefore, due to increase of the abundance of gas phase in the flow direction and the effect of pressure on the gas phase, the changes of flow characteristics are increased along the annulus in the flow direction.

Also, the effects of injected gas and liquid flow rates on the hydrostatic term of pressure are greater than its effect on the hydrodynamic term. So, in the lower part of the annulus, where the hydrostatic term is the predominant pressure term, the effect of these two parameters is greater than the well head.

By changing the choke pressure at the wellhead, the pressure will change equally along the entire length of the annulus. But due to decrease of the total pressure in the flow direction, the order of choke pressure compared to the total pressure becomes larger in the flow direction. So, the effects of the choke pressure on the annulus flow characteristics are increased in the flow direction. In summary, the obtained results shown that

1. For a constant operational parameters, the rate of changes of flow characteristics, including the volume fractions and velocities of different phases in the wellhead area was higher than the characteristics change in the bottom hole area. In other words, the changes of flow characteristics, including volume fractions and phase velocities are increased along the annulus in the flow direction.
2. The effects of injected gas flow rate on the flow characteristics in the bottom-hole area was greater than its effects in the wellhead area. In fact, the effects of injected gas flow rate on the flow characteristics are reduced along the annulus in the flow direction.
3. The effects of injected liquid flow rate on the flow characteristics are decreased along the annulus in the flow direction. Actually, the effects of injected liquid flow rate on the flow characteristics in the bottom-hole area were tangible, but its effects in the wellhead area are not sensible.
4. The effects of choke pressure on the flow characteristics are increased along the annulus in the flow direction. In fact, the changes of the flow characteristics due to the choke pressure variation in the wellhead area were higher than its changes in the bottom-hole area.

Nomenclature

A	Cross sectional area
BHP	Bottom hole pressure
F	Force
K_{Gin}	Mass flow rate of the inlet gas to the annulus
K_{Lin}	Mass flow rate of the inlet liquid to the annulus
K_{Sin}	Mass flow rate of the inlet cuttings to the annulus
M	Molar mass
P	Pressure
P_{ik}	Phase pressure
P_{R}	Reservoir pressure
t	Time
u	velocity
V_D	Drilling velocity
x	Flow direction
Z	Compersability factor
Greek symbols	
α	Volume Fraction
μ	Dynamic viscisity
ρ	density
Subscript	
G	Gas phase
L	Liquid phase
S	Solid phase
i	Node number
w	Wall
g	Gravity
v	Virtual

References

[1] Lorentzen, R.J., Fjelde, K.K., Froyen, J., Lage, A.C., Naevdal, G. and Vefring, E.H., 2001, January. Under-balanced drilling: Real time data interpretation and decision support. In SPE/IADC drilling conference. Society of Petroleum Engineers. https://doi.org/10.2118/67693-MS.

[2] Lorentzen, R.J., Fjelde, K.K., Froyen, J., Lage, A.C., Naevdal, G. and Vefring, E.H., 2001, January. Under-balanced and low-head drilling operations: Real time interpretation of measured data and operational support. In SPE Annual Technical Conference and Exhibition. Society of Petroleum Engineers. https://doi.org/10.2118/71384-MS.

[3] Lorentzen, R.J., Naevdal, G. and Lage, A.C., 2003. Tuning of parameters in a two-phase flow model using an ensemble Kalman filter. International Journal of Multiphase Flow, 29(8), pp.1283-1309. https://doi.org/10.1016/S0301-9322(03)00088-0.

[4] Vefring, E.H., Nygaard, G., Fjelde, K.K., Lorentzen, R.J., Naevdal, G. and Merlo, A., 2002, January. Reservoir characterization during underbalanced drilling: Methodology, accuracy, and necessary data. In SPE Annual Technical Conference and Exhibition. Society of Petroleum Engineers. https://doi.org/10.2118/77530-MS.

[5] Vefring, E.H., Nygaard, G.H., Lorentzen, R.J., Naevdal, G. and Fjelde, K.K., 2006. Reservoir characterization during underbalanced drilling (UBD): Methodology and active tests. SPE Journal, 11(02), pp.181-192. https://doi.org/10.2118/77530-MS.

[6] Fan, J., Gao, C., Taihe, S., Liu, H. and Yu, Z., 2001, January. A comprehensive model and computer simulation for underbalanced drilling in oil and gas wells. In SPE/ICoTA Coiled Tubing Roundtable. Society of Petroleum Engineers. https://doi.org/10.2118/68495-MS.

[7] Perez-Tellez, C., 2003. Improved Bottom Hole Pressure Control for Underbalance Drilling Operation (Ph. D. thesis). Louisiana State University.

[8] Perez-Tellez, C., Urbieta-Lopez, A., Miller, A. and Banda-Morato, R.G., 2003, January. Bottomhole Pressure Measurements: Indispensable Tool for Optimizing Underbalanced Drilling Operations. In Offshore Technology Conference. Offshore Technology Conference. https://doi.org/10.4043/15061-MS.

[9] Fadairo, A.S. and Falode, O.A., 2009, January. Effect of drilling cuttings transport on pressure drop in a flowing well. In Middle East Drilling Technology Conference & Exhibition. Society of Petroleum Engineers. https://doi.org/10.2118/125707-MS.

[10] Yan, T., Wang, K., Sun, X., Luan, S. and Shao, S., 2014. State-of-the-art cuttings transport with aerated liquid and foam in complex structure wells. Renewable and Sustainable Energy Reviews, 37, pp.560-568. https://doi.org/10.1016/j.rser.2014.05.047

[11] Ghobadpouri, S., Hajidavalloo, E. and Noghrehabadi, A.R., 2017. Modeling and simulation of gas-liquid-solid three-phase flow in under-balanced drilling operation. Journal of Petroleum Science and Engineering, 156, pp.348-355. https://doi.org/10.1016/j.petrol.2017.06.015.

[12] Wei, N., Xu, C., Meng, Y., Li, G., Ma, X. and Liu, A., 2018. Numerical simulation of gas-liquid two-phase flow in wellbore based on drift flux model. Applied Mathematics and Computation, 338, pp.175-191. https://doi.org/10.1016/j.amc.2018.03.067

[13] Li, X., Ma, H., Zhao, H., Gao, D., Lu, B., Ding, S., Gong, D. and Ma, Z., 2020. Study on the model for predicting maximum allowable measured depth of a horizontal well drilled with underbalanced operation. Journal of Petroleum Science and Engineering, 191, p.107104.https://doi.org/10.1016/j.petrol.2020.107104.

[14] Evje, S. and Flåtten, T., 2003. Hybrid flux-splitting schemes for a common two-fluid model. Journal of Computational Physics, 192(1), pp.175-210. https://doi.org/10.1016/j.jcp.2003.07.001.

[15] Hatta, N., Fujimoto, H., Isobe, M. and Kang, J.S., 1998. Theoretical analysis of flow characteristics of multiphase mixtures in a vertical pipe. International Journal of Multiphase Flow, 24(4), pp.539-561. https://doi.org/10.1016/S0301-9322(97)00074-8.

[16] Jahangiri, M. and Delbari, O., 2020. Heat Transfer Correlation for Two Phase Flow in a Mixing Tank. Journal of Heat and Mass Transfer Research, 7(1), pp.1-10. https://doi.org/10.22075/jhmtr.2020.17712.1232.

[17] Falavand Jozaei, A., Tayebi, A., Shekari, Y. and Ghafouri, A., 2017. Numerical simulation of transient natural gas flow in pipelines using high order DG-ADER scheme. Journal of Heat and Mass Transfer Research, 4(1), pp.35-43. https://doi.org/10.22075/jhmtr.2016.497.

[18] Dranchuk, P.M. and Abou-Kassem, H., 1975. Calculation of Z factors for natural gases using equations of state. Journal of Canadian

Petroleum Technology, 14(03). https://doi.org/10.2118/75-03-03.

[19] Bratland, O., 2010. Pipe flow 2: multi-phase flow assurance.

[20] Boyun, G., William, C. and Ali Ghalambor, G., 2007. Petroleum production engineering: a computer-assisted approach.

[21] Khezrian, M., Hajidavalloo, E. and Shekari, Y., 2015. Modeling and simulation of under-balanced drilling operation using two-fluid model of two-phase flow. Chemical Engineering Research and Design, 93, pp.30-37. https://doi.org/10.1016/j.cherd.2014.05.007.

[22] Lage, A.C. and Time, R.W., 2000, January. An experimental and theoretical investigation of upward two-phase flow in annuli. In SPE Asia Pacific Oil and Gas Conference and Exhibition. Society of Petroleum Engineers. https://doi.org/10.2118/64525-MS.